THE JOURNAL OF PHYSICAL CHEMISTRY B LETTERS

2006, *110,* 20098−20101
Published on Web 09/20/2006

Aromatic Superclusters from All-Metal Aromatic and Antiaromatic Monomers, $[Al_4]^{2-}$ and $[Al_4]^{4-}$

Sairam S. Mallajosyula, Ayan Datta, and Swapan K. Pati*

Theoretical Sciences Unit and the DST Unit on Nanoscience, Jawaharlal Nehru Center for Advanced Scientific Research, Jakkur P.O., Bangalore, India

Received: July 28, 2006; In Final Form: September 6, 2006

Calculations on the structures of dimers of all-metal aromatic and anti-aromatic molecules such as (Al_4^{2-}) and (Al_4^{4-}) reveal that, unlike their organic counterparts such as benzene and cyclobutadiene which form π-stacked complexes, these molecules form new clusters with no reminiscence of the original units. These clusters have a very large binding energy and can be further stabilized through charge-balance by counterions and solvents.

Intermolecular interactions between aromatic systems have been extensively studied during the past two decades, both experimentally and theoretically.[1−4] The importance of the noncovalent $\pi-\pi$ attractive interactions has been stressed in many fields ranging from molecular biology[5−7] to material sciences.[8,9] These weak interactions influence the structural and electronic properties of many organic and inorganic systems. The best known example of stacking interaction is between the nucleic acid bases that control the three-dimensional structure of DNA and its functions.[1−7] π-Stacking interactions also play a vital role in forming crystals of aromatic organic molecules and extended structures of hybrid organic−inorganic open-framework materials such as zeolites.[1−7] Benzene is often chosen as the model system for studying the $\pi-\pi$ interactions.[10−13] Detailed potential energy surface (PES) calculations for π stacks show the presence of a local minimum in the PES which favors the formation of π stacks in aromatic molecules over the nascent molecule. However, accurate determination of the binding energies for such π-stacked systems is a formidable task due to the limitations of the popular nonlocal functionals such as B3LYP, PW91, and PBE, etc. within the density functional theory (DFT) formalism to account for dispersion interactions. Calculations within the wave function methods, such as the coupled-cluster methods and MP2 (Møller−Plesset perturbation) level, being very expensive, are restricted to small systems only. However, the recent development of the dispersion-corrected DFT (DFT-D) appears very promising.[14]

In a similar context, the past few years have witnessed numerous reports of aromaticity and anti-aromaticity in metallic clusters.[15−17] Molecules such as Al_4^{2-} and Al_4^{4-} have been reported as aromatic and antiaromatic, respectively.[18−20] The additional photoelectron spectroscopic experiments support the computed structures. However, an unambiguous characterization of the systems is elusive due to the poor separation of the $\sigma-\pi$ orbitals in these all metal clusters. This has resulted in debates over whether the molecules are σ-aromatic or π-antiaromatic.[21,22] The complete characterization of these species will be confirmed only after successful crystal structure determination and charge density/atoms-in-molecules (AIM) characterizations.[23] To this regard, we have recently suggested a synthesis route for the stabilization of an all-metal antiaromatic molecule via complexation with a transition metal and their reaction intermediates.[24,25]

Thus, it would be very interesting to investigate whether these all-metal aromatic/anti-aromatic molecules also form π-stacked dimers. In fact, the possibility of fusion of all-metal clusters has been already predicted by Corbett and Seo[15(b)] and also by Kuznetsov et al. for Al_3^- dimer to form Al_6^{2-}.[16(d)] In this communication, we compare and contrast the nature of intermolecular interactions between the all-metal species and their closest organic counterparts. We find that the nature of intermolecular interactions is entirely different for these two classes of systems. While, the organic aromatic/anti-aromatic dimers are stabilized through weak dispersion forces, the all-metal systems form larger superclusters with very high binding energies. The monomers lose their structure completely in these superclusters. In fact, within these superclusters, each monomer cluster acts as a superatom, leading to the formation of highly stable three-dimensional structures.

We consider $[Al_4]^{2-}$ and $[Al_4]^{4-}$ as the monomers for modeling the aromatic and anti-aromatic stacked dimers, respectively. Our choice is based on well established theoretical and experimental characterization of $[Al_4]^{2-}$ and $[Al_4]^{4-}$.[17−20] The Gaussian 03 program[26] was used for the ab inito molecular orbital calculations. Electron correlation was accounted for using the second-order Møller−Plesset perturbation method (MP2)[27,28] at the 6-31+G(d,p) basis set level. The choice of the method is based on the success of MP2 electron correlation in describing stacking interactions in organic systems. Nucleus-independent chemical shift (NICS)[29] calculations are performed to characterize the aromatic/anti-aromatic nature of the adducts.

In Figure 1 we show the optimized geometries of C_6H_6, C_4H_4, $[Al_4]^{2-}$, and $[Al_4]^{4-}$. Upon optimization, we find the geometries of $[Al_4]^{2-}$ and $[Al_4]^{4-}$ to be square and rhombus, respectively. As expected from the aromaticity criteria, $[Al_4]^{2-}$ is square with all equivalent bond lengths and thus has 0 BLA (bond length

* Corresponding author. Fax: +91-080-22082767; Tel: +91-080-22082839; E-mail: pati@jncasr.ac.in

10.1021/jp064821n CCC: $33.50 © 2006 American Chemical Society

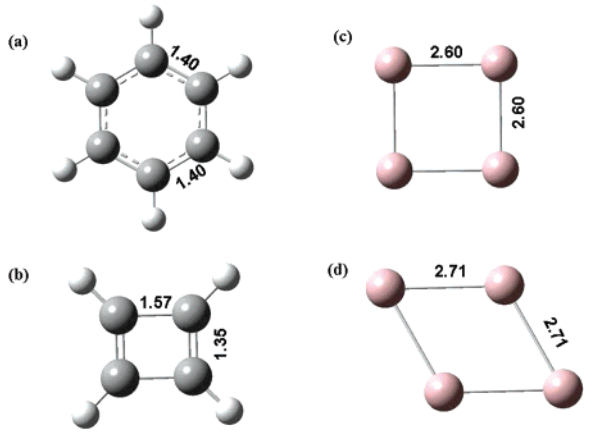

Figure 1. Optimized geometries of the aromatic and anti-aromatic systems: (a) C_6H_6, (b) C_4H_4, (c) $[Al_4]^{2-}$, and (d) $[Al_4]^{4-}$. The bond lengths are reported in Å. Color code: black, carbon; white, hydrogen; pink, aluminum.

alternation). However, the case of $[Al_4]^{4-}$ is interesting because, although it does not undergo rectangular Jahn−Teller distortion as in C_4H_4, there is a diamond type distortion that is well-known for four membered heteroatomic rings such as $B_2N_2H_4$ and $P_2N_2F_4$ (see Supporting Information for Molecular orbital analysis of Al_4^{4-}).[30] NICS, calculated at the center of each ring, are −9.695 ppm, +31.462 ppm, −53.557 ppm, and −3.087 ppm for C_6H_6 , C_4H_4 , $[Al_4]^{2-}$, and $[Al_4]^{4-}$, respectively.

A negative NICS indicates that the corresponding structure is aromatic, while a positive NICS reveals anti-aromatic character. However, we stress that the small negative NICS value found for $[Al_4]^{4-}$ is due to the poor $\sigma-\pi$ separation and may not indicate aromaticity as such.

Next, we optimized the dimer structures of C_6H_6 , C_4H_4, $[Al_4]^{2-}$, and $[Al_4]^{4-}$, respectively. In Figure 2 we show the optimized geometries corresponding to the minimum energy. We find that the optimized geometry of C_6H_6 corresponds to the well characterized slipped parallel π-stack (perpendicular distance, $d = 3.62$ Å). The geometry of C_4H_4 corresponds to a completely slipped parallel π-stacked dimer $d = 2.96$ Å. Very surprisingly, however, the all-metal systems, $([Al_4]^{2-})_2$ and $([Al_4]^{4-})_2$, form compact clusters.

We calculate the NICS at the molecular center as well as at the ring centers to characterize the aromatic/antiaromatic nature of these stacks. These values are reported in Table 1. The NICS values indicate that π interactions stabilize the stacked complexes. For $[C_4H_4]_2$, the individual rings retain the anti-aromatic character. However, the molecular center is essentially nonaromatic. Thus, a π-stacking interaction removes the antiaromatic character of the otherwise unstable anti-aromatic molecules. For $([Al_4]^{2-})_2$ and $([Al_4]^{4-})_2$ one cannot define two ring centers but the molecular center shows substantial aromatic character as the NICS value at the molecular center is substantially negative. In fact, the large gain in the diamagnetic ring current is the result of the formation of a single molecular species, stabilizing the hexagonal bipyramidal structure of $([Al_4]^{2-})_2$ and the distorted cubane type structure of $([Al_4]^{4-})_2$. Thus, the main point is that through the formation of superclusters, the antiaromatic destabilization of the all-metal systems can be removed (the charge delocalization over the entire supercluster is also evident from the natural population analysis as provided in the Supporting Information).

The potential energy surfaces (PES) for the systems are analyzed to understand the stability of the dimers. The energies at each configuration are determined by varying the perpendicular distance between the two monomer rings. For the $(Al_4)_2$ clusters, a pseudo ring center is used to calculate the perpendicular ring−ring distance (see Supporting Information for the structures). The PES for all the systems are plotted in Figure 3.

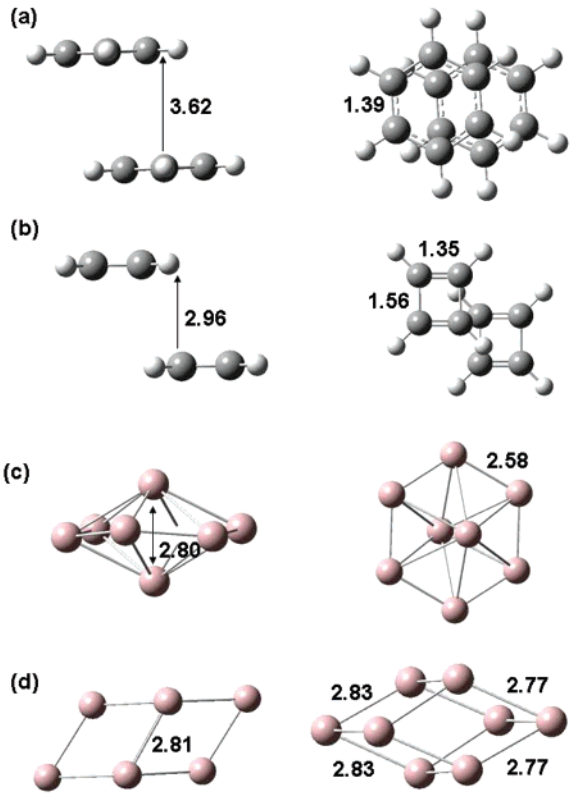

Figure 2. Optimized geometries of the aromatic and anti-aromatic dimers (side view and top view): (a) C_6H_6 stack, (b) C_4H_4 stack, (c) $[[Al_4]^{2-}]_2$ cluster, and (d) $[[Al_4]^{4-}]_2$ cluster. The bond lengths and distances are reported in Å. Color code: black − carbon; white − hydrogen; pink − aluminum.

TABLE 1: NICS Values (in ppm) for the Optimized Geometries at the Molecular Center and Ring Centers

	NICS (ppm)	
system	molecular center	ring centers
C_6H_6 stack	−11.74	−10.89 and −10.89
C_4H_4 stack	−0.749	30.973 and 30.972
$[Al_4]^{2-}$ cluster	−63.607	
$[Al_4]^{4-}$ cluster	−45.649	

We find that for the organic systems $(C_6H_6)_2$ and $(C_4H_4)_2$ there exists a shallow minimum corresponding to the optimized geometry but for $([Al_4]^{2-})_2$ and $([Al_4]^{4-})_2$, there exists a very deep minimum corresponding to the optimized geometry. Also note that, while for the organic dimers, the dissociation limit is reached as we approach larger separation distances, this is not the case for the all-metal systems. This is due to longer Al−Al bonds in Al_4 complexes as compared to C−C bonds in organic molecules such as C_6H_6.

The stabilization energy (ΔE) is calculated as the energy difference between the dimer and the monomer: $\Delta E = E(\text{dimer}) - 2 \times E(\text{monomer})$. Note that this energy is corrected for the basis-set superposition error (BSSE) through counterpoise (CP) correction scheme.[31] For the organic systems $(C_6H_6)_2$ and $(C_4H_4)_2$, we find the stabilization energy (ΔE) to be −2.23 kcal/mol and −3.52 kcal/mol, respectively. The negative value for the stabilization energy corresponds to the formation of a stable dimer structure. However, for the all-metal systems, ΔE are 89.96 and 616.98 kcal/mol for $([Al_4]^{2-})_2$ and $([Al_4]^{4-})_2$,

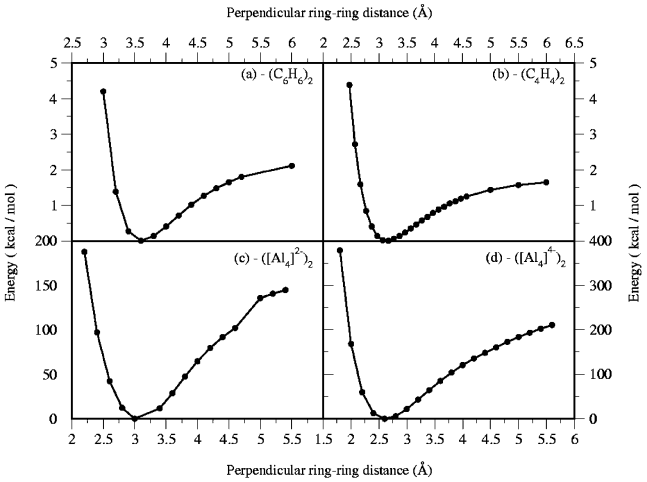

Figure 3. PES for the systems under study (a) C_6H_6 stack, (b) C_4H_4 stack, (c) $([Al_4]^{2-})_2$ cluster, and (d) $([Al_4]^{4-})_2$ cluster. The perpendicular ring−ring distances are reported in Å and energy is reported in kcal/mol.

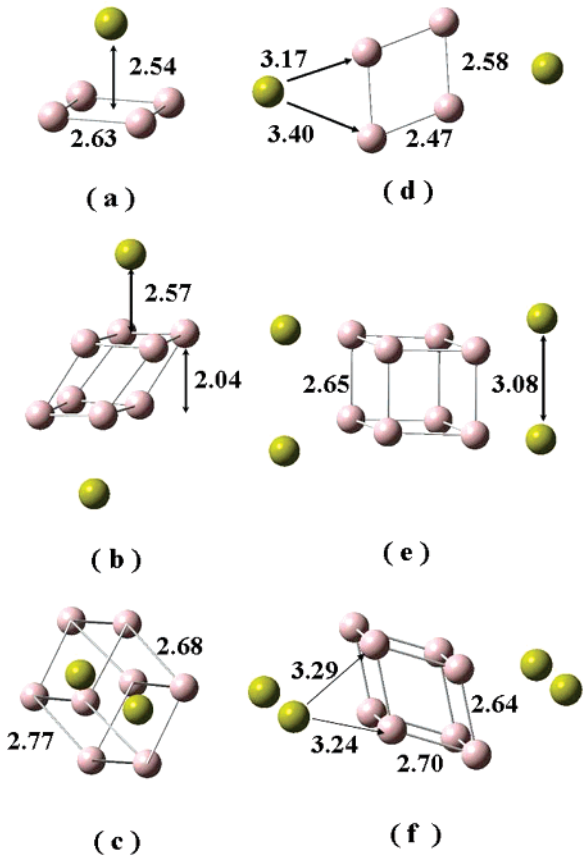

Figure 4. Optimized geometries of the aromatic and anti-aromatic metal chelated neutral species: (a) $[Al_4]^{2-}$ Ca^{2+}, (b) $[[Al_4]^{2-}]_2$ $(Ca^{2+})_2$ side view, (c) $[[Al_4]^{2-}]_2$ $(Ca^{2+})_2$ top view, (d) $[Al_4]^{4-}$ $(Ca^{2+})_2$, (e) $[[Al_4]^{4-}]_2$ $(Ca^{2+})_4$ side view, and (f) $[[Al_4]^{4-}]_2$ $(Ca^{2+})_4$ top view. The bond lengths and distances are reported in Å. Color code: pink − aluminum, yellow − calcium.

respectively. Thus, there is destabilization of the dimer as compared to the free monomer. However, from Figure 3, it is clear that the all-metal systems possess low energy structures due to the formation of larger clusters.

The apparent destabilization of the superclusters of $[Al_4]^{2-}$ and $[Al_4]^{4-}$ is due to the fact that while C_6H_6/C_4H_4 are neutral, their Al-analogues have formal negative charges (2 and 4 formal negative charges for $[Al_4]^{2-}$ and $[Al_4]^{4-}$, respectively). This introduces an effective Coulombic destablization compared to the small gain achieved through dispersion forces. To remove the Coulombic repulsions due to the large formal negative charges, we solvate the optimized stacked geometries in water within the polarizable continuum model (SCRF calculations). The large dielectric continuum of water reduces the electrostatic repulsions and stabilizes the stacked geometries ($\Delta E(([Al_4]^{2-})_2)$ = −62.07 kcal/mol; $\Delta E(([Al_4]^{4-})_2)$ = −119.41 kcal/mol).

Another process to overcome the interference associated with excess charge is to neutralize the all-metal aromatic and anti-aromatic systems by chelating them with the appropriate number of electropositive metal ions required to neutralize the systems. We consider a dipositive metal ion like Ca^{2+} as the neutralizing charge and perform geometry optimization at the same level of theory as discussed above. The structures are shown in Figure 4. We calculate the stabilization energy (ΔE) using the same scheme as defined earlier. The corresponding stabilization energies (ΔE) for $([Al_4]^{2-}$ $Ca^{2+})_2$ and $([Al_4]^{4-}$ $(Ca^{2+})_2)_2$ are found to be −131.59 kcal/mol and −114.49 kcal/mol, respectively. The negative value of ΔE and the large magnitude of the same indicates that the superclusters are substantially stable. For an understanding of the nature of interactions between the individual monomers in the clusters, we have investigated the molecular orbitals in the superclusters. Interestingly, we find that the MOs of the supercluster are highly delocalized with intermixing of the σ-electrons of the rings and formation of strong σ-bonds (see Supporting Information for the frontier orbitals). This explains the large stability of the all-metal superclusters as compared to only weak π-interacting cases for the organic counterparts.

In conclusion, we have shown for the first time, unlike their organic counterparts, dimers of all-metal aromatic/anti-aromatic clusters form extremely stable superclusters. In fact, recent calculations for Al_{13}^- clusters by Khanna and co-workers indicate the propensity of Al atoms to form compact clusters.[32] To this regard, we conjecture that the Al_8 clusters are aromatic and should be ideal candidates for experimental isolation through mass-spectrometric measurements or crystallization. Recent experimental realization of an Al_8 cubane-like supercluster (similar to Figure 4, structure (c)) supports our conjecture.[33]

Acknowledgment. S.S.M. and A.D. acknowledge support from CSIR India for JR and SR fellowships, respectively. S.K.P. thanks DST and CSIR for funding.

Supporting Information Available: Frontier orbital plots, full Gaussian reference, natural population analysis, and dissociation scheme of the all-metal clusters. This material is available free of charge via Internet at http://pubs.acs.org.

References and Notes

(1) Kwang, S. K.; Tarakeshwar, P.; Lee, J. Y. *Chem. Rev.* **2000**, *100*, 4145−4185.
(2) Meyer, E. A.; Castellano, R. K.; Diederich, F. *Angew. Chem., Int. Ed.* **2003**, *42*(11), 1210−1250.
(3) Muller-Dethlefs, K.; Hobza, P. *Chem. Rev.* **2000**, *100*, 143−168.
(4) Sponer, J.; Leszczynski, J.; Hobza, P. *Bioploymers* **2002**, *61*, 3−21.
(5) McGaughey, G. B.; Gagné, M.; Rappé, A. K. *J. Biol. Chem.* **1998**, *273*(25), 15458−15463.
(6) Kool, E. T. *Annu. Rev. Biophys. Biomol. Struct.* **2001**, *30*, 1−22.
(7) Elstner, M.; Hobza, P. Frauenheim, T.; Suhai, S.; Kaxiras, E. *J. Chem. Phys.* **2001**, *114*(12), 5149−5155.
(8) Rao, C. N. R.; Natarajan, S.; Vaidhyanathan, R. *Angew. Chem., Int. Ed.* **2004**, *43*(12), 1466−1496.
(9) Tournus, F.; Latil, S.; Heggie, M. I.; Charlier, J. C. *Phys. Rev. B* **2005**, *72*, 075431−075435.
(10) Hobza, P.; Selzle, H. L.; Schlag, E. W. *J. Phys. Chem.* **1996**, *100*(48), 18790−18794.

(11) Tsuzuki, S.; Honda, K.; Uchimaru, T.; Mikami, M.; Tanabe, K. *J. Am. Chem. Soc.* **2002**, *124*(1), 104−112.

(12) Sinnokrot, M. O.; Valeev, E. F.; Sherrill, C. D. *J. Am. Chem. Soc.* **2002**, *124*(36), 10887−10893.

(13) Sinnokrot, M. O.; Sherrill, C. D. *J. Phys. Chem. A* **2004**, *108*(46), 10200−10207.

(14) Piacenza, M.; Grimme, S. *ChemPhysChem* **2005**, *6*, 1554.

(15) (a) Li, X.; Kuznetsov, A. E.; Zhang, H.-F.; Boldyrev, A. I.; Wang, L.-S.; *Science* **2001**, *291*, 859−861. (b) Corbett, J. D.; Seo, D.-K. *Science* **2001**, *291*, 841−842.

(16) (a) Li, X.; Zhang, H.-F.; Wang, L.-S.; Kuznetsov, A. E.; Cannon, N. A.; Boldyrev, A. I. *Angew. Chem., Int. Ed.* **2001**, *40*(10), 1867−1870. (b) Todorov, L.; Sevov, S. C. *Inorg. Chem.* **2005**, *44*, 5361. (c) Todorov, L.; Sevov, S. C. *Inorg. Chem.* **2006**, *45*, 4478. (d) Kuznetsov, A. E.; Boldyrev, A. I.; Zhai, H.-J.; Li, X.; Wang, L.-S. *J. Am. Chem. Soc.* **2002**, *124*, 11791−11801.

(17) (a) Kuznetsov, A. E.; Corbett, J. D.; Wang, L.-S.; Boldyrev, A. I. *Angew. Chem., Int. Ed.* **2001**, *40*(18), 3369−3372.

(18) Kuznetsov, A. E.; Boldyrev, A. I.; Li, X.; Wang, L.-S. *J. Am. Chem. Soc.* **2001**, *123*, 8825−8831.

(19) Kuznetsov, A. E.; Birch, K.; Boldyrev, A. I.; Li, X.; Zhai, H.; Wang, L.-S. *Science* **2003**, *300*, 622−625.

(20) (a) Tsipis, C. A. *Coord. Chem. Rev.* **2005**, *249*, 2740−2762. (b) Boldyrev, A. I.; Wang, L.-S. *Chem. Rev.* **2005**, *105*, 3716−3757.

(21) (a) Santos, J. C.; Andres, J.; Aizman, A.; Fuentealba, P. *J. Chem. Theor. Comput.* **2005**, *1*, 83. (b) Santos, J. C.; Tiznado, W.; Contreras, R.; Fuentealba, P. *J. Chem. Phys.* **2004**, *6*, 256.

(22) (a) Datta, A.; Pati, S. K. *J. Chem. Theor. Comput.* **2005**, *1*, 824−826. (b) Lin, Y.-C.; Juselius, J.; Sundholm, D.; Gauss, J. *J. Chem. Phys.* **2005**, *122*, 214308.

(23) (a) *Atoms in Molecules: A Quantum Theory*; Bader, R. F. W., Ed.; Clarendon Press: Oxford, U. K., 1995. (b) Ranganathan, A.; Kulkarni, G. U. *Proc. Indian Acad. Sci. Chem. Sci.* **2003**, *115*, 637.

(24) Datta, A.; Pati, S. K. *J. Am. Chem. Soc.* **2005**, *127*, 3496−3500.

(25) Datta, A.; Pati, S. K. *Chem. Commun.* **2005**, 5032−5034.

(26) Frisch, M. J.; Trucks, G. W.; Schlegel, H. B.; Scuseria, G. E.; Robb, M. A.; Cheeseman, J. R.; Montgomery, J. A., Jr.; Vreven, T.; Kudin, K. N.; Burant, J. C.; Millam, J. M.; Iyengar, S. S.; Tomasi, J.; Barone, V.; Mennucci, B.; Cossi, M.; Scalmani, G.; Rega, N.; Petersson, G. A.; Nakatsuji, H.; Hada, M.; Ehara, M.; Toyota, K.; Fukuda, R.; Hasegawa, J.; Ishida, M.; Nakajima, T.; Honda, Y.; Kitao, O.; Nakai, H.; Klene, M.; Li, X.; Knox, J. E.; Hratchian, H. P.; Cross, J. B.; Bakken, V.; Adamo, C.; Jaramillo, J.; Gomperts, R.; Stratmann, R. E.; Yazyev, O.; Austin, A. J.; Cammi, R.; Pomelli, C.; Ochterski, J. W.; Ayala, P. Y.; Morokuma, K.; Voth, G. A.; Salvador, P.; Dannenberg, J. J.; Zakrzewski, V. G.; Dapprich, S.; Daniels, A. D.; Strain, M. C.; Farkas, O.; Malick, D. K.; Rabuck, A. D.; Raghavachari, K.; Foresman, J. B.; Ortiz, J. V.; Cui, Q.; Baboul, A. G.; Clifford, S.; Cioslowski, J.; Stefanov, B. B.; Liu, G.; Liashenko, A.; Piskorz, P.; Komaromi, I.; Martin, R. L.; Fox, D. J.; Keith, T.; Al-Laham, M. A.; Peng, C. Y.; Nanayakkara, A.; Challacombe, M.; Gill, P. M. W.; Johnson, B.; Chen, W.; Wong, M. W.; Gonzalez, C.; Pople, J. A. *Gaussian 03*, revision B.05; Gaussian, Inc.: Wallingford, CT, 2004.

(27) Møller, C.; Plesset, M. S. *Phys. Rev.* **1934**, *46*, 618.

(28) Head-Gordon, M.; Pople, J. A.; Frisch, M. J. *Chem. Phys. Lett.* **1988**, *153*, 503.

(29) Schleyer, P. v. R.; Maerker, C.; Dransfeld, A.; Jiao, H.; Eikema-Hommes, N. J. R. v. *J. Am. Chem. Soc.* **1996**, *118*, 6317.

(30) Rehaman, A.; Datta, A.; Sairam, S. M.; Pati, S. K. *J. Chem. Theor. Comput.* **2006**, *2*, 30.

(31) Boys, S. F.; Bernardi, F. *Mol. Phys.* **1970**, *19*, 553.

(32) Bergeron, D. E.; Roach, P. J.; Castleman, A. W. Jr.; Jones, N. O.; Khanna, S. N. *Science* **2005**, *307*, 231. (b) Bergeron, D. E.; Castleman, A. W. Jr.; Morisato, T.; Khanna, S. N. *Science* **2004**, *304*, 84.

(33) Kratochvil, J.; Necas, M.; Petricek, V.; Pinkas, J. *Inorg. Chem.* **2006**, *45*, 6562.